



Contents lists available at [ScienceDirect](#)

Zoology

ZOOLOGY

journal homepage: www.elsevier.com/locate/zool

Jumping sans legs: does elastic energy storage by the vertebral column power terrestrial jumps in bony fishes?

Miriam A. Ashley-Ross^{a,*}, Benjamin M. Perlman^a, Alice C. Gibb^b, John H. Long Jr.^c

^a Department of Biology, Wake Forest University, Box 7325, Winston-Salem, NC 27109, USA

^b Department of Biological Sciences, Northern Arizona University, 617 S. Beaver St., Flagstaff, AZ 86011, USA

^c Department of Biology, Vassar College, Olmsted Hall of Biological Science 317, Poughkeepsie, NY 12604, USA

ARTICLE INFO

Article history:

Received 24 August 2013
Received in revised form 11 October 2013
Accepted 14 October 2013
Available online xxx

Keywords:

Terrestrial locomotion
Axial skeleton
Vertebral spines
Flexural stiffness
Elastic recoil

ABSTRACT

Despite having no obvious anatomical modifications to facilitate movement over land, numerous small fishes from divergent teleost lineages make brief, voluntary terrestrial forays to escape poor aquatic conditions or to pursue terrestrial prey. Once stranded, these fishes produce a coordinated and effective “tail-flip” jumping behavior, wherein lateral flexion of the axial body into a C-shape, followed by contralateral flexion of the body axis, propels the fish into a ballistic flight-path that covers a distance of multiple body lengths. We ask: how do anatomical structures that evolved in one habitat generate effective movement in a novel habitat? Within this context, we hypothesized that the mechanical properties of the axial skeleton play a critical role in producing effective overland movement, and that tail-flip jumping species demonstrate enhanced elastic energy storage through increased body flexural stiffness or increased body curvature, relative to non-jumping species. To test this hypothesis, we derived a model to predict elastic recoil work from the morphology of the vertebral (neural and hemal) spines. From ground reaction force (GRF) measurements and high-speed video, we calculated elastic recoil work, flexural stiffness, and apparent material stiffness of the body for *Micropterus salmoides* (a non-jumper) and *Kryptolebias marmoratus* (adept tail-flip jumper). The model predicted no difference between the two species in work stored by the vertebral spines, and GRF data showed that they produce the same magnitude of mass-specific elastic recoil work. Surprisingly, non-jumper *M. salmoides* has a stiffer body than tail-flip jumper *K. marmoratus*. Many tail-flip jumping species possess enlarged, fused hypural bones that support the caudal peduncle, which suggests that the localized structures, rather than the entire axial skeleton, may explain differences in terrestrial performance.

© 2013 Elsevier GmbH. All rights reserved.

1. Introduction

1.1. The axial skeleton in vertebrate locomotion

Flexion of the vertebral column is a fundamental aspect of locomotor movements in the vast majority of living vertebrates. Side-to-side, or lateral, axial undulation is used by most extant fishes to produce forward propulsion through the fluid medium in which they live (e.g., Sfakiotakis et al., 1999), and dorsoventral axial undulation drives locomotion for many aquatic mammals (e.g., Fish, 1998). Even among terrestrial vertebrates, where limbs are often the structures that interact directly with the substrate to produce propulsive ground reaction forces (GRF), axial movements play a significant role in locomotion (Daan and Belterman, 1968; Hildebrand, 1985; Frolich and Biewener, 1992; Ritter, 1992; Ashley-Ross, 1994; Ryerson, 2013). For limbed vertebrates

(Tetrapoda), when axial flexion in either plane is appropriately timed with limb extension, stride length is increased – which will increase locomotor speed for a given cycle frequency. In tetrapods that have secondarily lost their limbs (caecilians, snakes, legless lizards), the body axis can produce a range of undulatory locomotor modes. Snakes, for example, generate novel axial movements that create a range of locomotor behaviors, including such extremes as sidewinding and concertina locomotion (Gans, 1962). Thus, vertebrates from diverse lineages employ a homologous structure – the vertebral column, its associated axial musculature, and its spinal neural circuitry – to produce an astounding range of behaviors across physically divergent habitats.

In aquatic chordates, undulatory traveling waves are the best-studied cyclic axial-based locomotor behavior. Because these propulsive waves of bending power swimming in larval ascidians (McHenry et al., 2003), adult lancelets (Webb, 1973), hagfish (Long et al., 2002), and lamprey (Root et al., 2007), axial undulation is likely the ancestral locomotor behavior for the Vertebrata (Koob and Long, 2000). Hence when salamanders (Frolich and Biewener, 1992), sirens (Gillis, 1997), snakes (Jayne, 1985), and alligators

* Corresponding author. Tel.: +1 336 758 5529.

E-mail address: rossma@wfu.edu (M.A. Ashley-Ross).

(Fish and Lauder, 2013) swim via lateral undulation, they harness a conserved locomotor system driven by spinal central pattern generators that activate segmental muscles to produce bending moments that flex the body, and, in so doing, transfer momentum to the surrounding water (Tytell et al., 2010).

Of unsteady, transient aquatic locomotor behaviors, the fast-start escape response (C-start) is the most intensively studied. An aquatic fast-start is triggered by the firing of neuromasts (vibration sensors) connected to the VIIIth cranial nerve, which in turn recruit reticulospinal neurons (of which the Mauthner neuron is the largest), resulting in motor output that bends the body at a high rate and to a large magnitude; those axial motions move the animal away from the stimulus (Zottoli and Faber, 2000; Hale et al., 2002). The initial phase of the fast-start, stage 1, is a C-shaped bend away from the stimulus that is generated by synchronous contraction of the axial musculature on the concave side of the bend (Jayne and Lauder, 1993). Stage 1 moves the head away from the stimulus, and the fish's turning angle can range from very slight to 30–180° away from the threat (Domenici and Blake, 1997; Eaton et al., 2001). The next phase, stage 2, is generated by an anterior-to-posterior traveling wave of activation of the contralateral musculature (Domenici and Blake, 1997; Eaton et al., 2001), which generates a propulsive stroke of the tail back to the opposite side, propelling the fish in a trajectory away from the threat (Tytell and Lauder, 2002).

1.2. Elastic energy in the axial musculoskeletal system

Both on land and in the water, and in steady and transient movements, the axial body imparts momentum to the environment via bending. In addition to providing the muscular power that drives bending, the body can also store and release elastic energy (Long and Nipper, 1996; Long, 1998). Two components of the body are prime candidates for elastic springs: (i) the vertebral column, including the vertical septum in which it is encased, and (ii) the other tissues of the body, including muscle, the integument, and other connective tissues. Many vertebrates appear to use the vertebral column to store and recover elastic energy (blue marlin: Long, 1992; eels: Long, 1998; hagfish: Long et al., 2002; sharks: Long et al., 2011b), although the vertebral columns of longnose gar (Long et al., 1996) and striped bass (Nowroozi and Brainerd, 2013) lack sufficient flexural stiffness and in vivo strain to store energy in this manner. When considered as individual elements or as a unit, the other tissues that constitute the axial body can also add flexural stiffness to that provided by the vertebral column, as has been demonstrated in pumpkinseed sunfish (Long et al., 1994; Summers and Long, 2006), hagfish (Long et al., 2002), and longnose gar (Long et al., 1996), and has been suggested for plethodontid salamanders (Ryerson, 2013).

The ability of muscle, which is by volume the single largest element of the axial body, to store and return elastic energy can be enhanced via actuation by the nervous system. In eels, the passive flexural stiffness of the body can be tripled with appropriately timed muscle activity (Long, 1998). One method by which activated muscles may stiffen the body is by increasing intramuscular pressure. During stage 1 of the fast-start of bowfin, *Amia calva*, and the bichir, *Polypterus palmus*, the intramuscular pressure of the body increases rapidly, and then stays elevated during stage 2 while the tightly bent body straightens (Westneat et al., 1998). Similarly, active stiffening during steady swimming may potentially enable fishes to tune the resonance properties of their bodies and thereby minimize the energetic costs of bending.

A causal link between stiffness and swimming performance has been demonstrated in freely swimming robotic fish propelled by undulating bodies or tails of varying stiffness (McHenry et al., 1995; Long et al., 2011a,b). As the apparent material stiffness (or Young's modulus) of the tail increases, so, too, does the rate at

which steady swimming speed increases with increasing tail beat frequency (Long et al., 2011a,b). Likewise, as the apparent material stiffness of the tail increases, so, too, does peak acceleration that can be achieved at a given rate of flexion (Long et al., 2011a). In self-propelled robotic models of pumpkinseed sunfish, increases in the body's apparent material stiffness increase the body's propulsive wavelength, which, all else equal, increases the robot's swimming speed (McHenry et al., 1995). However, a higher magnitude of stiffness is not always better. In a self-propelled sunfish tail robot, two optimal stiffnesses exist – one that maximizes the production of thrust and another that maximizes lift (Esposito et al., 2012). Moreover, the optimal stiffness for producing the maximum steady swimming speed, as determined in force-coupled computer simulations of undulatory robots (Long et al., 2010), is also of intermediate magnitude.

Because some locomotor performance optima occur at intermediate levels of flexural body stiffness, and the optimal stiffnesses vary depending on the desired performance, it seems clear that trade-offs exist. Taken to one extreme, if the body is too stiff relative to the muscle power available to bend it, then the animal may be unable to produce undulatory waves, create the rapid body bending required for maneuvering, and make the body deformations required to store elastic energy. On the other hand, if the body is too flexible, an animal may not be able to achieve high speeds, rapid accelerations, or store appreciable elastic energy. These trade-offs are evident in computational simulations of swimming fish, where intermediate stiffnesses are optimal for rapid acceleration and high steady swimming speeds (Tytell et al., 2010; Bhalla et al., 2013). Similarly, intermediate tail stiffnesses produce the greatest stride lengths in self-propelled robotic fish during steady swimming (Long et al., 2011b). Intermediate stiffnesses are likely optimal because they enable a structure to deform sufficiently to produce effective displacement and allow bent elements to store elastic energy.

1.3. The tail-flip jump

Because the axial musculoskeletal system of fishes has been under selection for locomotor performance in the water for hundreds of millions of years, we anticipate that their bodies are adapted to the biophysical forces of the aquatic environment. However, many fishes occupy habitats in near-shore littoral zones and may encounter the terrestrial realm via incidental or deliberate stranding on land (Mast, 1915; Bayliss, 1982; Soares and Bierman, 2013). Once on land, these aquatic vertebrates must cope with the physical demands of the terrestrial environment, including the low density of the surrounding air and the full force of gravity. Fully aquatic fishes that become stranded are compelled to use a morphology that has been adapted for locomotion in one environment to locomote in a drastically different environment and in a fundamentally different manner.

Remarkably, many fully aquatic fishes from the Teleostei produce a stereotyped, coordinated, and highly effective response to stranding: the tail-flip jump (Gibb et al., 2011, 2013). The tail-flip is an unsteady locomotor behavior characterized by the following sequence of events (Fig. 1; see movies 1–5 in the supplementary online Appendix). The tail-flip typically begins with the fish lying on its side (although some species begin the movement from a prone position); in response to a negative stimulus or of its own volition, the fish will peel its head away from the substrate, curling the anterior body up and over the caudal peduncle in a C-shaped preparatory phase (stage 1). Once the center of mass (COM) has passed over the caudal peduncle, the vertebral column straightens, pressing the caudal peduncle and tail fin against the substrate (stage 2). As a result of these movements, the fish launches off of

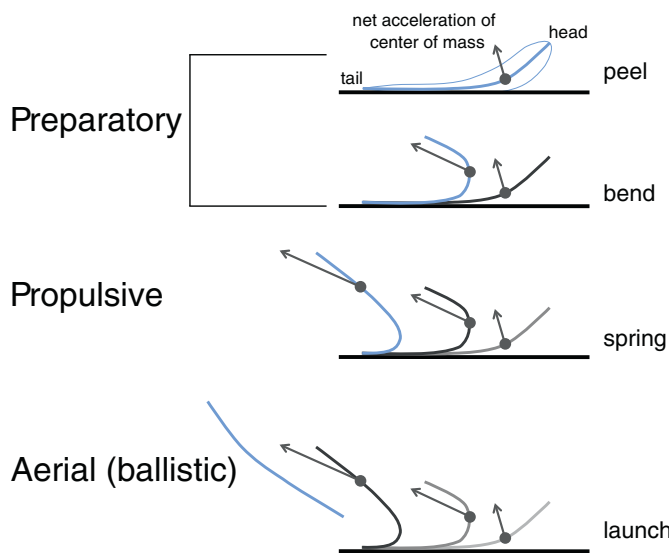


Fig. 1. The tail-flip jump is characterized by three stereotyped phases. During the preparatory phase, the fish peels its anterior body off of the substrate and bends the head over the caudal peduncle, thus storing elastic strain energy in the bent vertebral column and connective tissues. During the propulsive phase, the fish straightens the vertebral column, releasing stored elastic energy. As a result, the fish springs off of the caudal peduncle and propels itself into the aerial (or ballistic) phase of the jump. The blue line represents the midline of the fish and the thin blue outline in the top panel illustrates the outline of the fish's body.

the tail into a ballistic aerial phase wherein it travels multiple body lengths before landing (Fig. 1).

While the pattern of body bending is superficially similar to that of the aquatic fast-start, the timing of movements during the two behaviors is markedly different: the terrestrial behavior is slower than the aquatic behavior and the initial bending phase takes much longer (approximately 5 times longer; Gibb et al., 2011). Perhaps even more importantly, the physical interaction between the fish's body and the surrounding environment is, by necessity, different in the two behaviors. In an aquatic C-start, the body is not under gravitational load, and it generates thrust by accelerating the surrounding fluid. In a terrestrial tail-flip jump, the body must overcome its gravitational load, and it generates thrust by pushing against an unyielding substrate. Because the terrestrial substrate does not yield, we would expect, for a given amount of force or moment produced, that the body would bend more than in an aquatic fast-start.

We have documented the tail-flip jump in disparate teleost taxa: representatives of the Cypriniformes, Esociformes, Gobiiformes, Blennioidei, Atherinomorpha, and Perciformes. Tail-flip jumps are used in different ecological contexts depending on the species: (i) in response to accidental stranding to return to the water (Ashley-Ross, Gibb, Perlman, pers. obs.), (ii) to escape poor water conditions (Davis et al., 1990), (iii) to escape predators (Bayliss, 1982), or (iv) to pursue terrestrial prey (Huehner et al., 1985). It is unclear whether the tail-flip is an ancestral behavior for the Teleostei (in which case the tail-flip is over 250 million years old; Gibb et al., 2013), or if it evolved multiple times. Independent of phylogenetic considerations, the tail-flip appears to be restricted to early life history stages or to species with small adult body sizes – perhaps because as body mass increases, mass-relative muscle force decreases (Carpenter-Carter et al., 2012).

Interestingly, not all teleost fish species can produce a tail-flip jump. Juvenile *Micropterus salmoides*, the largemouth bass, cannot produce a tail-flip jump, but instead generates a “thrash” – a movement also characterized by C-shaped axial bending (Gibb et al., 2013). Thrashing enables a stranded bass to propel itself into

the air, which can result in horizontal displacement of up to three body lengths. However, species that produce the tail-flip jump (e.g., *Gambusia affinis*, *Danio rerio* and *Kryptolebias marmoratus*) consistently move more than five body lengths as the result of a single tail-flip (Gibb et al., 2013). This occurs, in part, because the thrashing as seen in *M. salmoides* creates takeoff angles that propel fish vertically into the air, while tail-flipping creates takeoff angles that result in horizontal movement during ballistic flight (Gibb et al., 2013; Perlman et al., 2013; see movies 1–5 in the supplementary online Appendix).

What accounts for the differences among teleost taxa in terrestrial locomotor performance? One possibility is that tail-flip jumpers are able to modulate patterns of motor activity to produce effective movement in the terrestrial environment. Another possibility is that tail-flip jumping species have a body with mechanical properties better suited to the physical demands of the new environment. Indeed, effective terrestrial movements are likely to be a combination of both. However, we note that animals are known to minimize energetic costs by off-loading control of key behaviors from energetically expensive nervous systems to the intrinsic biomechanical interaction between body and environment (“morphological computation” sensu Pfeifer et al., 2006; Pfeifer and Bongard, 2007) because they get the physics for free, metabolically speaking. In addition, the reactions are fast because the physical interaction of body and world can generate rapid feedback, via the closed-loop, force-coupled, dynamic system that creates complex motor behaviors outside of the relatively slow control loop of the nervous system (Dickinson et al., 2000). Because of the clear benefits to off-loading aspects of locomotor behaviors to body–environment interactions, we posit that the axial anatomy of teleost fishes plays a key role in determining locomotor performance of fish on land.

1.4. Specific predictions

We test the hypothesis that morphology determines terrestrial locomotor performance in stranded teleosts. We do so by evaluating axial anatomy and locomotor performance in two ways. First, we evaluate the prediction that the physical structure (the architecture) of the vertebral column affects the body's flexural stiffness and determines the storage and release of elastic energy during jumping. To test this prediction, we examine five species that vary widely in their terrestrial locomotor performance. If there are no differences in the morphology of the axial skeleton among taxa with different levels of locomotor performance on land, then this prediction is refuted. Second, in two teleost species that have been selected to represent an excellent tail-flip jumper (*K. marmoratus*) and a non-jumper (*M. salmoides*, a “thrasher”), we calculate the flexural stiffness of the active body during take-off and the mechanical work done during elastic recoil from a combination of high-speed video and ground reaction force measurements. We expect that the excellent tail-flip jumper, when compared to the thrasher, will (i) produce faster take-off velocities, (ii) generate more elastic recoil work per unit body mass, and (iii) possess greater apparent material stiffness of the body.

1.5. Stiffness and elastic recoil in bending and jumping bodies

Based on the physics of going ballistic, we know that tail-flip jumpers accelerate their bodies while in contact with the ground to achieve a take-off velocity that generates a sufficient change in momentum to counteract the force of gravity. While jumping fish may power this transfer of momentum instantaneously using muscles, elastic recoil work, stored earlier from the mechanical work used to bend the body, could augment the on-going muscular work of jumping.

Given the presence of passive and active stiffness during the bending of fish bodies, it is highly likely that stiffness plays a role in tail-flip jumping, which involves high-amplitude bending of the body (Gibb et al., 2011). To bend a beam, mechanical work input, W_i (Nm), is required in proportion to the beam's flexural stiffness, EI_b (Nm^2):

$$W_i = EI_b l_b \kappa^2 \quad (1)$$

where l_b is the length of the beam (m) and κ is the curvature of the beam (m^{-1}). The work output, W_o , from the beam that is recovered as elastic recoil is the product of W_i and the beam's resilience, R , a non-dimensional number between 0 and 1.

Aspects of vertebral morphology that vary among species, and therefore may be a candidate for creating differences in the EI of the vertebral column, are the bony neural and hemal spines. In blue marlin, *Makaira nigricans*, the plate-like neural and hemal spines span the intervertebral joint and thus bend with the joint; they are responsible for a substantial proportion of the vertebral column's EI (Hebrank et al., 1990). However, the spines in most bony fish species, including those studied here, are slender rods rather than plates. In terms of the EI of the vertebral column, we hypothesize that the contribution is proportional to the effective axial length of the neural or hemal spine, l_e , which depends on its angle, α , relative to the long axis of the vertebral column, and its length, l_s :

$$l_e = l_s \cos \alpha \quad (2)$$

We can substitute Eq. (2) into Eq. (1), add resilience, R , and use the resulting equation to estimate the effect of changes in the vertebral spine morphologies, α and l_s , on the elastic work output, W_o :

$$W_o = REI_b l_s \cos \alpha \kappa^2 \quad (3)$$

To test our hypotheses, we measure the relative spine lengths and angles in the caudal vertebral columns of five species of teleost. We predict that those species with better terrestrial locomotor performance will have higher values of W_o , as estimated by morphology alone. Using high-speed video and ground reaction force measurements, we also measure independently EI and W_o of the whole, active body of the two species of the five with the most dramatic differences in terrestrial locomotor performance.

2. Materials and methods

2.1. Animals

Representatives of five teleost species were used for measurements of vertebral morphology. Individuals of a non-jumping species, juvenile largemouth bass, *M. salmoides* ($n=5$), were obtained from Carolina Biological Supply, Inc. (Burlington, NC, USA). Individuals of four tail-flip jumping species were obtained from a variety of sources. Mangrove rivulus, *K. marmoratus*, were collected by B.M.P. ($n=3$; see below for details), or obtained from a laboratory colony maintained by Dr. Ryan Earley at the University of Alabama ($n=1$). Zebrafish, *D. rerio*, were obtained from a commercial vendor ($n=4$). Western mosquitofish, *G. affinis*, were provided by the Arizona Game and Fish Department (Flagstaff, AZ, USA) ($n=6$). Female Siamese fighting fish, *Betta splendens*, were obtained from a commercial vendor ($n=4$). After they had been preserved in buffered formalin and then transferred to ethanol, the specimens were cleared and stained to identify bone and cartilage, following the methods of Dingerkus and Uhler (1977). The five species examined here represent one member of the Cypriniformes (*D. rerio*), two Cyprinodontiformes (*G. affinis* and *K. marmoratus*), and two Perciformes (*M. salmoides* and *B. splendens*).

Representatives of the two species with the most divergent terrestrial abilities were also used for live animal studies of locomotor

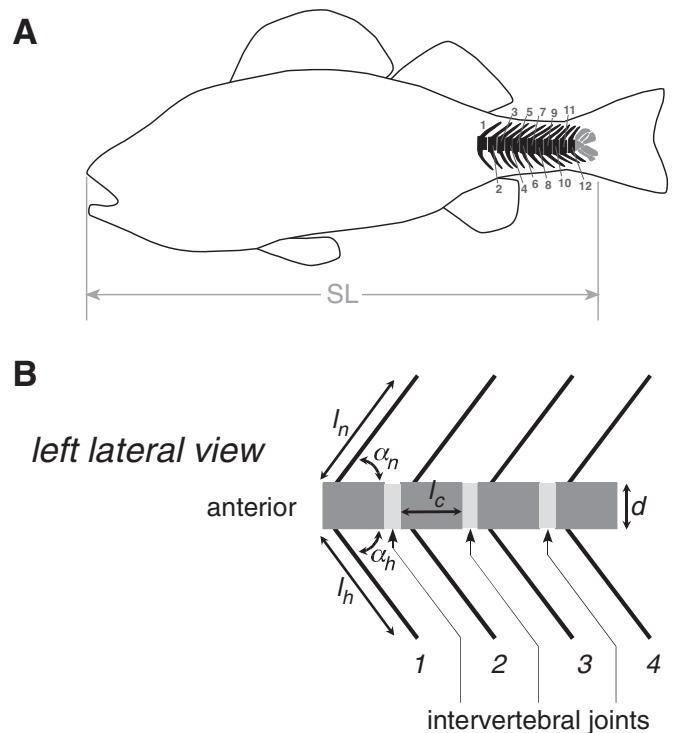


Fig. 2. (A) Morphological variables are measured from the 12 caudal-most vertebrae and then used as inputs for a model of elastic energy storage and release by the neural and hemal spines; to control for size differences among species, these measurements are standardized to the standard length (SL) of the fish. (B) Left lateral view of the vertebral column with four successive vertebrae and six morphometric variables: centrum length l_c , centrum depth d , length of the neural and hemal spines l_n and l_h , and the angle of the neural and hemal spines α_n and α_h .

mechanics. Live juvenile *M. salmoides* ($n=2$) were obtained from Carolina Biological Supply Co. (Burlington, NC, USA). Live adult *K. marmoratus* ($n=3$) were collected using cup traps (Taylor, 1990) in the Florida Keys, Florida, USA in June 2011 (SAL-09-1132B-SR, issued by the Florida Fish and Wildlife Conservation Commission to Dr. Ryan L. Earley), and on Long Caye, Lighthouse Reef Atoll, Belize (BAHA-IAHC-11.08-L009, issued by the Belize Agricultural Health Authority and Belize Fisheries Department to B.M.P.) in August 2011. Performance data (takeoff velocity, GRF) were collected during experimental trials for a related project at Clemson University (see Section 2.3). All procedures followed Wake Forest University IACUC protocol A11-134 and Clemson University IACUC protocol AUP 2013-018.

Although these represent limited numbers of animals, we are developing these methods de novo; data presented here demonstrate the feasibility of the new technique and provide sufficient statistical power to avoid type II errors (see Section 3.4).

2.2. Morphometrics

The following measurements were used to quantify differences in vertebral morphology in all five species: standard length, neural spine angle, neural spine length, hemal spine angle, hemal spine length, and the number of intervertebral joints crossed by each neural and hemal spine (Fig. 2). Measurements were made in ImageJ 1.47 (Rasband, 1997–2012) from digital photomicrographs (Leica stereomicroscope; Leica Microsystems, Wetzlar, Germany) taken for each specimen from a lateral view with a plastic ruler placed in the frame for scale. Spine angles were measured between the long axis of the vertebral centrum and a line connecting the tip of the spine with the center of its base, where it merged with the centrum. Spine length, l_s , was measured along the axis of the spine

from its base to the tip; the “segmented line” function in ImageJ followed any curves in the spine. Only the last 12 vertebrae (just anterior to the terminal, ural vertebra) were analyzed so as to avoid potential complications due to the presence of the median dorsal and anal fins adjacent to the more anterior vertebrae. Hypural morphology (size, degree of fusion) was also examined for all species. For locomotor mechanics, body mass, total length, and body width were measured as inputs for our model of the energy stored in the column and the flexural stiffness generated during terrestrial locomotor behaviors.

2.3. Locomotor mechanics

To measure GRF in the vertical, mediolateral, and anteroposterior planes during the behavioral response to stranding, a live fish was placed onto a custom-built multi-axis force plate (K&N Scientific, Guilford, VT, USA) covered with wetted bench-liner paper. Two synchronized high-speed digital video cameras (500 Hz) were used to record behaviors in lateral and dorsal views (Phantom v.4.1; Vision Research Inc., Wayne, NJ, USA). An LED light placed within the field of view of the digital camera flashed in synch with a 1.5 V pulse in the force trace to synchronize the GRF data and videos. Additional details of this procedure are given in Kawano and Blob (2013) and Butcher and Blob (2008). The vertical component of the GRF, F_g (N), of the lift-off phase was sampled at 5000 Hz with a low-pass filter (21 point moving average). Using finite differences, the instantaneous F_g was integrated over the time that the fish bent in contact with the ground, t (s), to yield the impulse, J (Ns), of the locomotor movement.

Takeoff velocity, U_t (m s^{-1}), was measured by digitizing the approximate position of the fish's COM in ImageJ 1.47. Because it served as a distinguishable landmark on the video, the pectoral girdle was used as a proxy for COM. The position of the pectoral girdle was digitized over four successive frames (interframe interval of 0.002 s): the first time point was the last frame in which the fish was still in contact with the force plate, just before it became a projectile, and the subsequent three points occurred when the fish was airborne. The U_t for each individual was the average of the three successive velocities along the ballistic trajectory.

2.4. Flexural stiffness and elastic recoil

To estimate relative differences in EI of the vertebral column caused by differences in the morphology of the neural and hemal spines, we used Eq. (3) to generate the following proportionality for an approximation of elastic work output, W'_0 :

$$W'_0 \propto I_s \cos \alpha \quad (4)$$

Because we are interested in differences in functional morphology across species, we normalized Eq. (4) by the standard length of the body, l , such that:

$$W^*_0 \propto \frac{W'_0}{l} \propto \frac{I_s}{l} \cos \alpha \quad (5)$$

Four aspects of morphology affect W^*_0 : the normalized neural and hemal spine lengths, and the angles of the neural and hemal spines to the long axis of the vertebral column (Fig. 2). The total W^*_0 for a section of vertebral column, $W^*_{o,total}$ – in our analysis the 12 vertebrae cranial to the ural vertebra of the caudal fin – is as follows:

$$W^*_{o,total} \propto \sum_1^{12} \left(\frac{I_s}{l} \cos \alpha \right)_{neural} + \sum_1^{12} \left(\frac{I_s}{l} \cos \alpha \right)_{hemal} \quad (6)$$

with these estimates, we use morphology to predict the relative differences among species in the mechanical behavior of the vertebral column as an elastic spring in jumping fishes.

Using data on the actual performance of two species, *K. marmoratus* and *M. salmoides*, we estimated the EI of the entire active body of the fish during a terrestrial locomotor behavior. It is important to note that EI is a composite variable; E is Young's modulus or material stiffness (Pa), and I is the second moment of area (m^4), a shape factor that accounts for the distribution of mass in the cross-section relative to the presumed neutral axis of bending.

We estimated EI of the entire active body of a jumping fish in two ways. First, we calculated the kinetic energy of the jump, K_E (in Joules):

$$K_E = m_b U_t^2 \quad (7)$$

where m_b (kg) is the mass of the fish's body. Setting Eq. (7) equal to Eq. (3) (Conte et al., 2010), we solved for EI_K , where the subscript K indicates this value is estimated from the kinetic energy of the jump:

$$EI_K = \frac{U_t^2 m_b}{\eta l_b \kappa^2} \quad (8)$$

where η is a transfer efficiency of unknown value (we assume 1 hereafter).

Second, we measured EI of the whole, active body as EI_F , where the subscript F indicates this value is estimated from F_g (N). The quotient of J and t yields the average \bar{F}_g produced, which, in turn, was used to calculate an average bending moment, M (Nm), causing the fish's maximum body curvature, κ :

$$M = \bar{F}_g r = EI_F \kappa \quad (9)$$

where r is the moment arm (m), here estimated as the radius of curvature of the body at maximal κ , and EI_F , according to beam theory, is the proportionality constant between M and κ in pure bending. Because r and κ are inversely proportional, we rearrange Eq. (9):

$$EI_F = \frac{\bar{F}_g}{\kappa^2} \quad (10)$$

Note that both EI_K and EI_F (Eqs. (8) and (10), respectively) are inversely proportional to the square of the maximal body curvature, κ .

To produce an estimate of the apparent E of the whole body, the quotient of EI and I can be taken, where I is calculated using an elliptical approximation of the thickest part of the body; hence, E so calculated is a conservative underestimate.

3. Results

3.1. Vertebral spine length and orientation

Vertebral spine length (Fig. 3), l_s , is anticipated to directly alter body stiffness (Eq. (3)). Based on our measurements, the non-jumper, *M. salmoides*, tends to have the shortest spines, though only *B. splendens* and *G. affinis* have noticeably longer spines than the rest (see Table S1 in the supplementary online Appendix).

For all five species examined, the angles α , made by the neural and hemal spines with the centrum axis become more acute in the vertebrae near the posterior end of the column (Fig. 4). Largemouth bass, *M. salmoides*, and zebrafish, *D. rerio*, appear to demonstrate the simplest relationship between spine angle and position, with a nearly linear decrease in angle from anterior to posterior occurring for both species. The other three species show either a decrease followed by stasis or an increase in angle (*G. affinis* and *B. splendens*) or little change in angle with position (*K. marmoratus*). We originally hypothesized that tail-flip jumpers would have

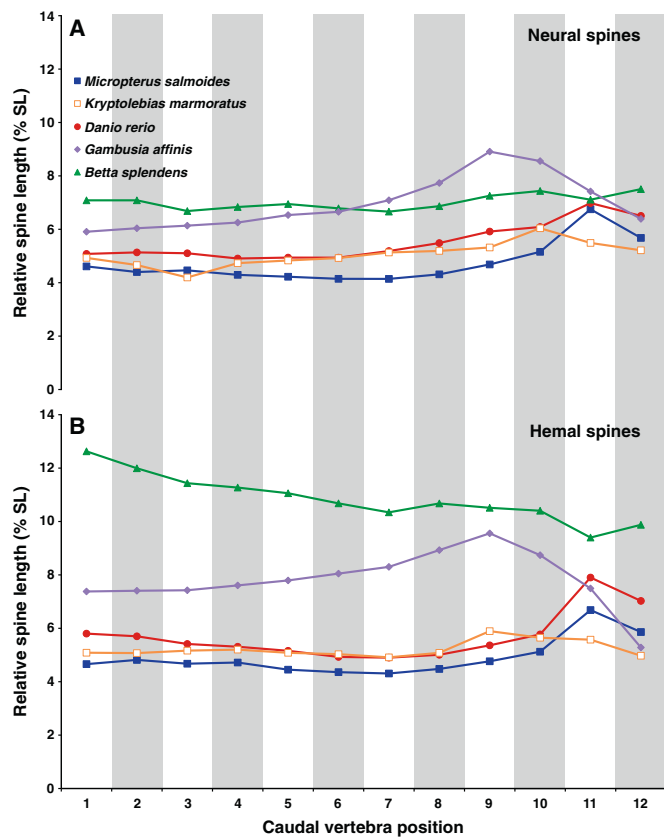


Fig. 3. Relative lengths (percentage of standard length, SL) of the (A) neural and (B) hemal spines of the last 12 vertebrae for the teleost species examined for this study. Error bars are not shown for clarity; standard deviations for each mean are given in Table S1 in the supplementary online Appendix.

more acute spine angles (relative to non-jumping species) because as spine angles α become more acute, the effective spine length increases (Eq. (2)). However, neural and hemal spine angles in tail-flip jumpers are either indistinguishable from, or greater than, those in the non-jumping species (*M. salmoides*), so this hypothesis was not supported.

Vertebral spine bending is also influenced by the number of intervertebral joints it spans; a spine that crosses two joints can be expected to bend more than a spine that crosses a single joint. The number of intervertebral joints spanned by the neural and hemal spines varies in a complex manner among the five species (Fig. 5). For all five species, the neural spines of vertebra #1 always cross a single joint, and the hemal spines also cross only a single joint in all species except in some specimens of *B. splendens*. In *M. salmoides*, the neural and hemal spines of vertebrae 2–6 also cross a single joint, then demonstrate inter-individual variation for the next few vertebrae, but then consistently span multiple joints for vertebrae 9–11. In *D. rerio*, spines also cross a single joint for vertebrae 2–7, then span 2 or sometimes 3 joints for the next several vertebrae. The posterior-most two vertebrae are invariant among species, with the penultimate vertebra's spines crossing the single joint available to it, and the next vertebra's spines crossing two joints. However, we note that in *K. marmoratus*, *G. affinis* and *B. splendens*, the neural and hemal spines begin crossing multiple joints in more anterior positions than in *M. salmoides* or *D. rerio* (Fig. 5). This suggests an increased potential for bending of the spines in those species, which should allow the vertebral spines of these species to store more elastic energy when the body is curved.

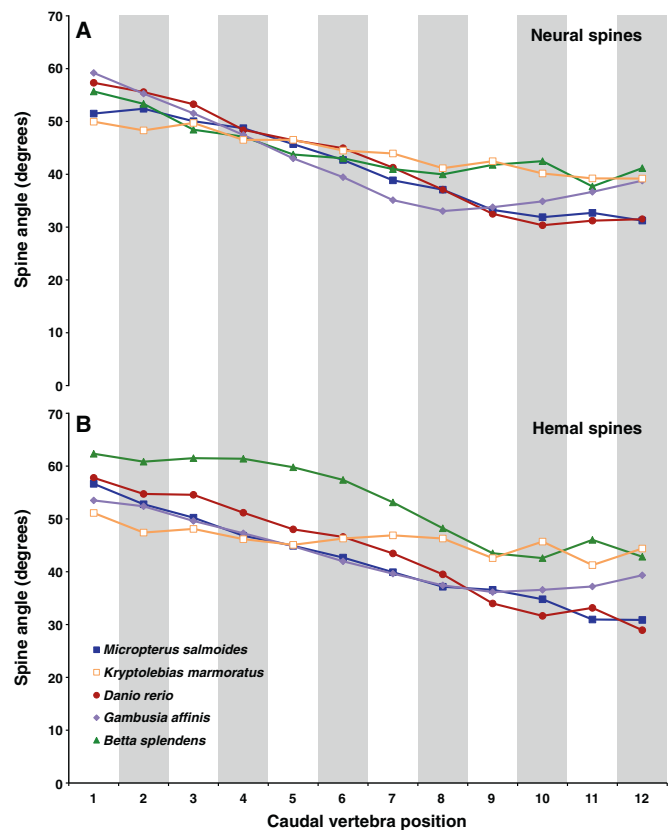


Fig. 4. Angles with the long axis of the vertebral column of the (A) neural and (B) hemal spines of the last 12 vertebrae for the species examined for this study. Error bars are not shown for clarity; standard deviations for each mean are given in Table S2 in the supplementary online Appendix.

3.2. Modeling energy storage by the neural and hemal spines

The morphology-based model presented here incorporates two key aspects of vertebral spine morphology, angle and length, α and l_s , respectively, to predict the relative potential for elastic energy storage in the 12 caudal-most vertebrae (Eq. (3)). The product of these two variables may be used as a proxy for work stored (Fig. 6). The same patterns are seen for all five species in both neural and hemal spines: work stored increases toward the tail. Contributions to work stored are approximately equal between neural and hemal spines, with the exception of *B. splendens*, where work stored in hemal spines is greater than that of neural spines. Totals summed over the 12 vertebrae are significantly different among species (one-way ANOVA, $F = 33.63$, $p < 0.00001$), being lowest in *M. salmoides* (total = 86.5 m; non-jumper) and highest in *B. splendens* (total = 136.0 m; tail-flip jumper). Surprisingly, values for *K. marmoratus* (total = 87.2 m; most proficient tail-flip jumper; Gibb et al., 2013) are quite close to those of *M. salmoides* (Fig. 6).

3.3. Variation in hypural anatomy

Among the five species examined, the hypural bones of the caudal fin differ in both number and relative size. *M. salmoides* and *D. rerio* have multiple, independently moveable hypurals (Fig. 7A and B). *K. marmoratus* and *G. affinis* have most or all of the hypurals fused into a single, centrally located plate that is likewise fused into the terminal vertebra (Fig. 7C and D); this is a defining characteristic of the Cyprinodontiformes (Costa, 1998, 2012; Parenti, 1981). Finally, individuals of *B. splendens* have large, expanded, partially fused hypural bones (Fig. 7E).

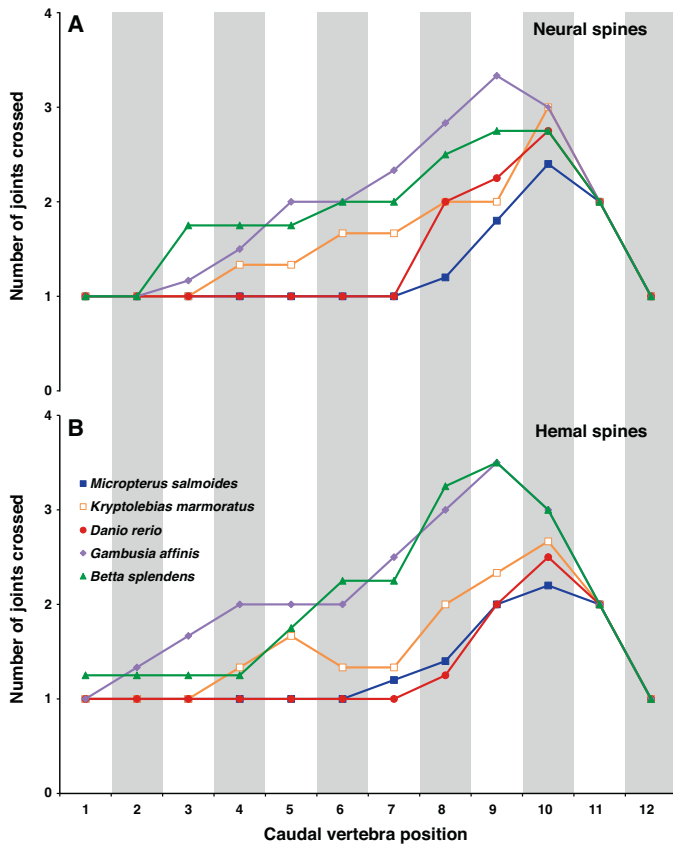


Fig. 5. Numbers of intervertebral joints crossed for the (A) neural and (B) hemal spines of the last 12 vertebrae for the species examined for this study. Error bars are not shown for clarity; standard deviations for each mean are given in Table S3 in the supplementary online Appendix.

3.4. Locomotor mechanics

Terrestrial behaviors in two species that are widely divergent in terrestrial locomotor ability, *M. salmoides* and *K. marmoratus* (Gibb et al., 2013), were used to calculate the dynamic flexural stiffness of the body and the work recovered via elastic recoil. Individuals of *K. marmoratus* always execute coordinated tail-flips that move them multiple body lengths as the result of a single effort (Fig. 8A–C). In contrast, individuals of *M. salmoides* appear unable to execute a tail-flip, instead producing a body-bending behavior termed thrashing (sensu Gibb et al., 2013) when stranded on land; a thrashing behavior may be initiated either away from (Fig. 8D–F), or toward (Fig. 8G–I), the substrate. The takeoff velocity, U_t , and body mass, m_b , which are used to calculate El_K (Eq. (8)), are both significantly different (all results given here are from two sample, two-tailed, unequal variance t -tests, with $\alpha = 0.05$) for *M. salmoides* and *K. marmoratus* ($p = 0.0022$ and $p < 0.001$, respectively) and inversely proportional in the two species (Fig. 9A and B).

It is notable that both methods produce the same prediction of dynamic flexural stiffness for a given species, i.e., the two independently derived estimates of El generated for a given species were not statistically different from one another ($p = 0.104$ and $p = 0.508$, *K. marmoratus* and *M. salmoides*, respectively). For *K. marmoratus*, the mean El with both methods pooled is $1.69 \times 10^6 \text{ N m}^2$ ($\pm 0.596 \times 10^6 \text{ SD}$); for *M. salmoides*, the mean El with both methods pooled is $21.56 \times 10^6 \text{ N m}^2$ ($\pm 12.124 \times 10^6 \text{ SD}$); these means are significantly different between species ($p = 0.010$; Fig. 9E). When El is normalized by the maximum l of the body, then the resulting mean apparent material stiffness, E , of the body is significantly different, with *M. salmoides* having a mean value of E nearly twice

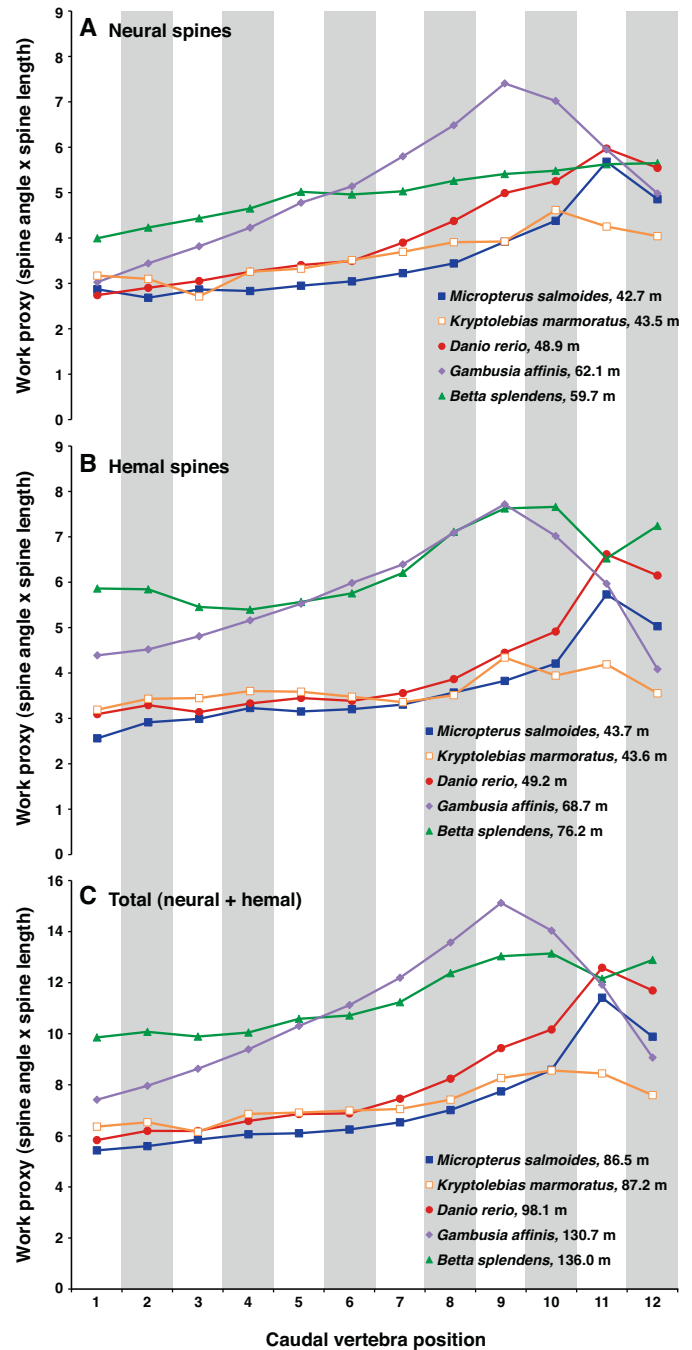


Fig. 6. Output from the model used to predict the elastic energy stored and released by the (A) neural and (B) hemal spines, and (C) their sum, for the last 12 vertebrae of *M. salmoides* (a non-jumper), *K. marmoratus*, *D. rerio*, *G. affinis*, and *B. splendens* (tail-flip jumpers). Numbers given in the lower right of every panel after the name of each species represent the summation for all vertebrae for the variable depicted in that panel. Error bars are not shown for clarity; standard deviations for each mean are given in Table S4 in the supplementary online Appendix.

that of *K. marmoratus* ($p = 0.033$; Fig. 9F). In contrast, although initial estimates of mechanical work output from elastic recoil yielded mean values that were significantly greater in *M. salmoides* than in *K. marmoratus* ($p = 0.013$; Fig. 9C), after W_0 is normalized by m_b , the two species are not significantly different from one another ($p = 0.148$; Fig. 9D).

The values for maximal overall curvature of the body, taken from high-speed video recordings (Fig. 8), were nearly twice as high in *K. marmoratus* relative to *M. salmoides* ($p < 0.001$), with means of

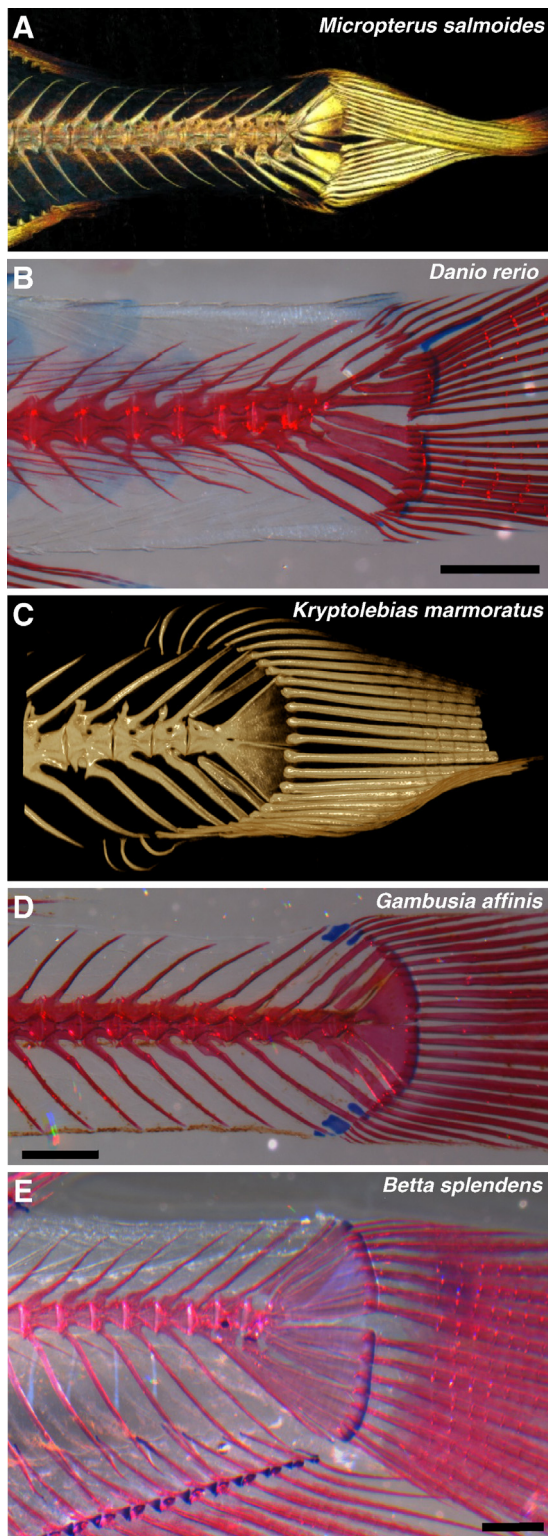


Fig. 7. Vertebral and hypural anatomy of the five species considered in this study (caudal end with peduncle and caudal fin rays to the right). (A) The non-jumper *M. salmoides* (micro-CT scan) reveals multiple, unfused hypural bones. (B) Tail-flip jumper *D. rerio* (cleared and stained specimen) likewise has unfused hypurals. Tail-flip jumpers (C) *K. marmoratus* (micro-CT scan), (D) *G. affinis* and (E) *B. splendens* (cleared and stained specimens) all demonstrate varying degrees of fusion of the hypurals into a plate-like structure. Scale bars = 1 mm.

104.2 m^{-1} and 49.3 m^{-1} , respectively. However, mean values of body length, l_b , were also different between species ($p < 0.001$), with means of 4.09 cm and 8.54 cm for *K. marmoratus* and *M. salmoides*, respectively. When the length-specific curvature was calculated as the non-dimensional product of κ and l_b , those differences disappeared ($p = 0.746$) and the mean curvature across both species was 4.2.

4. Discussion

4.1. Elastic energy storage by the axial skeleton

Because elastic energy storage and release enhances performance and efficiency in both aquatic and terrestrial locomotion for other vertebrate systems, we hypothesized that it would affect performance of terrestrial locomotion in small teleost fishes. Specifically, we expected that tail-flip jumping species would demonstrate greater body stiffness during the jump, and possess specific anatomical features of the posterior axial skeleton, including longer and more acutely angled neural and hemal spines, and expanded hypural bones. In five different species with varying terrestrial locomotor abilities, we considered the potential contribution of the morphology of the vertebral column to the body's flexural stiffness, EI , and the work output of elastic recoil, W_o . Further, we compared EI and W_o of the whole body measured in experiments in a non-jumper (thrasher), *M. salmoides*, and an excellent jumper, *K. marmoratus*. To our surprise, in neither case does EI or W_o of the vertebral column or the whole body explain the differences in jumping performance.

Equally surprising, vertebral spine angles and lengths measured from the most caudal vertebrae, and thus the work proxy used in the model, did not differ between *M. salmoides* and *K. marmoratus* (Figs. 3, 4 and 6). In fact, the work proxy values for these two species are the lowest among the five species examined, in spite of demonstrated differences in terrestrial locomotor ability across these taxa (Gibb et al., 2013). Therefore, differences in vertebral morphology do not wholly drive terrestrial locomotor ability. Based on whole-body jumping mechanics, when normalized for body size and I , the only difference between *M. salmoides* and *K. marmoratus* was that the former (a non-jumper) was substantially stiffer than the latter (a tail-flip jumper, Fig. 9F).

4.2. The caudal peduncle and tail fin in terrestrial locomotion

Is it possible our a priori expectation was incorrect and effective locomotor movement on land actually requires decreased stiffness in the caudal region? Fish that produce coordinated jumps on land appear to undergo substantial bending at the caudal peduncle, suggesting that there may be decreased stiffness in this region of the axial skeleton. Gibb et al. (2011) compared aquatic C-starts with terrestrial jumps of *G. affinis* and *D. rerio* and found that both species form a "C"-shape during the escape response and during the middle phase of the terrestrial jump behavior. However, just before take-off during a tail-flip jump, *G. affinis* (a more proficient jumper in terms of generating an effective take-off angle) forms a J-shaped curve at the posterior end of the axial skeleton. This bending allows the hypural plate to be pressed effectively against the ground and generates a take-off angle of $\sim 45^\circ$. In contrast, *D. rerio* does not produce this J-bend and has a near vertical takeoff angle (Gibb et al., 2011) – which could potentially reduce the ability of *D. rerio* to move efficiently across long distances. Because our model uses overall body bending, it does not take into account potential localized bending and/or mechanical interactions with the substrate, such as might occur between the caudal peduncle or fin and the ground.

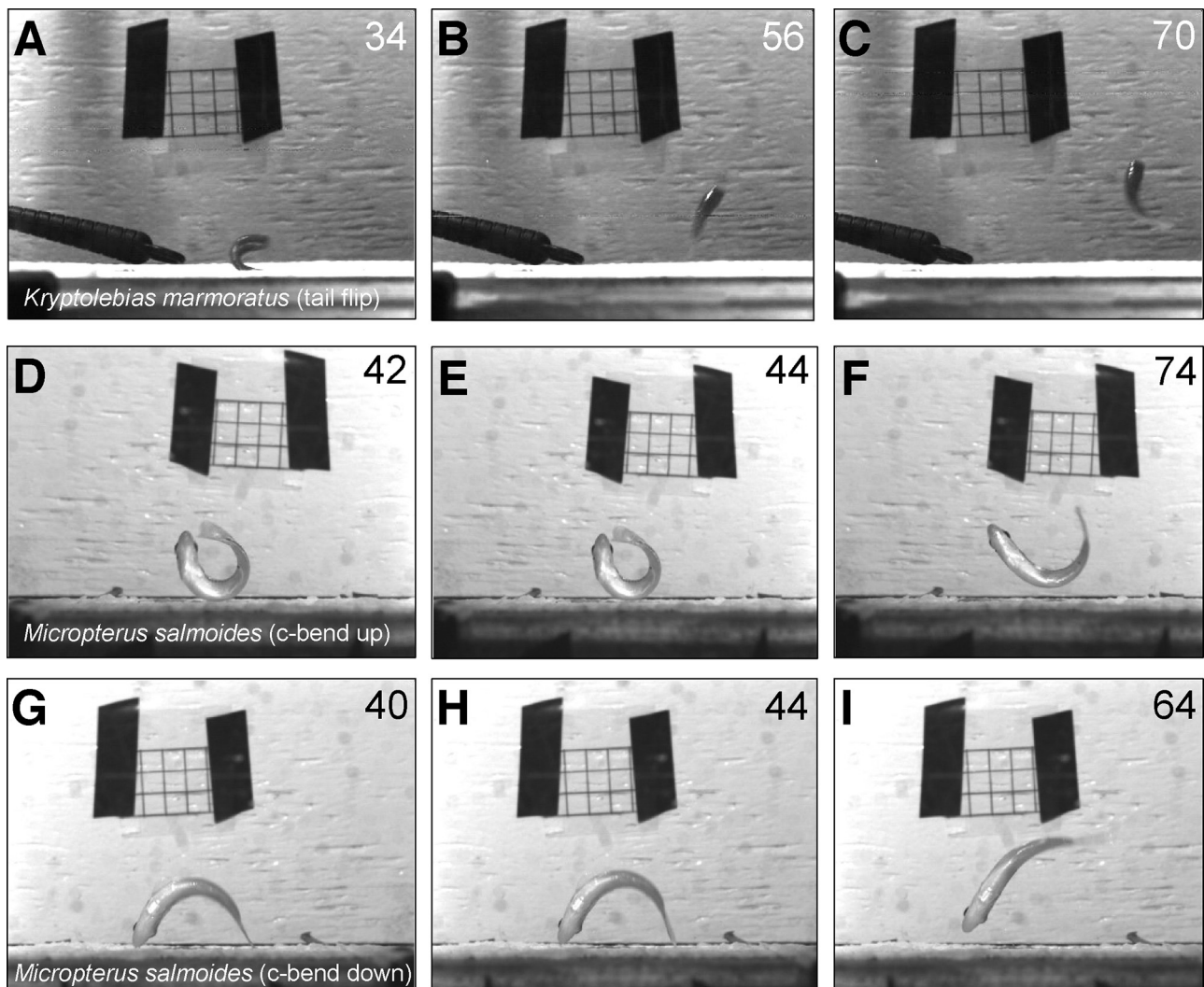


Fig. 8. (A–C) *K. marmoratus* are proficient tail-flip jumpers, while *M. salmoides* have two ways to produce a thrashing behavior that generates little horizontal displacement: (D–F) c-bend up, (G–I) c-bend down. Individual frames have been selected from high-speed video sequences to demonstrate movements produced by the two species when placed on land: maximum body curvature (left column), the frame immediately before takeoff (center column), and the ballistic phase (right column). Images extracted from the high-speed video sequences were flipped horizontally so that initial head position is consistently to the left; images were also adjusted to enhance brightness and contrast, but no other digital manipulations were performed. Numbers in each frame represent time (in ms) elapsed from time zero (not shown), defined as the frame immediately preceding the first discernible movement. Scale is given in each image by a 1 cm × 1 cm grid.

In addition, the mechanical properties of the caudal peduncle and fin, which are the structures responsible for imparting force to the substrate and propelling the fish into the air, are still unknown. Despite its lower overall body stiffness, *K. marmoratus* has a significantly greater take-off velocity than *M. salmoides* (Fig. 9A), which suggests that higher magnitude forces must be imparted to the ground at take-off through the caudal peduncle + fin. Three of the tail-flip jumpers examined here (*K. marmoratus*, *B. splendens* and *G. affinis*) demonstrated more robust and fused hypural bones than *M. salmoides* (Fig. 7), and such expanded hypural support should provide greater stability and stiffness to the tail and facilitate a controlled and energetic launch. Similar hypural morphology might be expected in *G. affinis* and *K. marmoratus* due to shared ancestry (Fig. 7C and D; Costa, 1998, 2012; Parenti, 1981); however, *M. salmoides* and *B. splendens* are both perciform fishes, yet these two species do not share hypural morphology (Fig. 7A and E). Rather, the adept tail-flip jumper *B. splendens* has hypurals that are expanded and partially fused, while the tail of *M. salmoides* is composed of many individual hypural elements, which could influence the ability of *M. salmoides* to effectively impart posteriorly directed forces at takeoff.

4.3. Aquatic vs. terrestrial locomotor performance

During the tail-flip jump, the head and anterior body undergo extreme bending, relative to the rest of the body (Gibb et al., 2011), and this flexion appears to be necessary to accelerate the COM up and off of the substrate (Fig. 1). However, it is possible that the ability to produce anterior flexion is reduced in fish with body forms that facilitate aquatic swimming performance. One aspect of body form that correlates with steady swimming performance is fineness ratio (body length divided by the length of the greatest dimension in an orthogonal direction); the fineness ratio of the non-jumping species *M. salmoides* is 4.3, which is similar to the hypothetical ideal for steady swimming (4.5) proposed by Webb (1975). We posit that the deep body profile of the anterior body of *M. salmoides* may streamline the overall body shape and enhance their ability to swim steadily at high velocities, but restrict their ability to produce the coordinated anterior-to-posterior wave of extreme bending during the preparatory phase that is characteristic of effective tail-flip jumpers. We also note that tail-flip jumping species tend to have a shallower, longer body profile and high fineness ratios (Gibb et al., 2013), which supports the overarching hypothesis that body

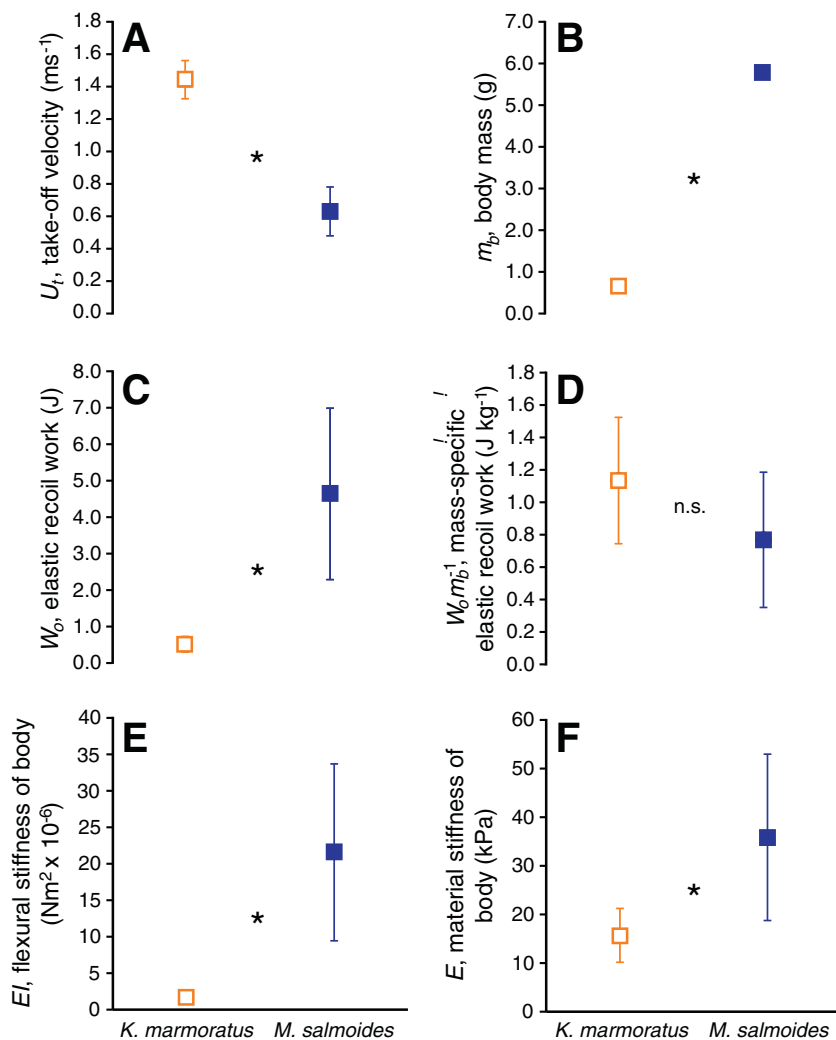


Fig. 9. Model outputs for *K. marmoratus* and *M. salmoides*, the two species at the extremes of the terrestrial locomotor performance spectrum in the present study. (A) Takeoff velocities are greater in *K. marmoratus* than in *M. salmoides*. (B) Adult *K. marmoratus* tested had significantly lower body mass than the juvenile *M. salmoides*. (C) *K. marmoratus* generates significantly less elastic recoil work than *M. salmoides*. (D) Because both species generate the same mass-specific elastic recoil work, the difference in elastic recoil work between the two species appears to be explained by size difference. (E) Flexural stiffness of the active bodies is significantly less in *K. marmoratus* than in *M. salmoides*. (F) Even when normalized by the second moment of area, I , the material stiffness of the active body in individuals of *K. marmoratus* is significantly less than that in individuals of *M. salmoides*.

forms in jumping species have been altered to facilitate the production of effective terrestrial movements. However, although a high fineness ratio may assist flexibility at the anterior end of the body to facilitate jumping, we hypothesize that species with high fineness ratios experience reduced performance during key aquatic locomotor behaviors.

4.4. Future directions

In this study, we document variation in the morphology of the posterior axial skeleton in five teleost species with different terrestrial locomotor abilities and then use these data as input parameters for a mathematical model to predict elastic energy storage and release by the vertebral column. We also derive values for whole-body flexural stiffness and material stiffness from performance measures taken from live fish. Somewhat surprisingly, neither the morphology-based model nor E_i derivations explained observed differences in jumping performance across species. However, it is important to note that neither approach considers, or in fact can capture, temporal variation in the mechanical properties of the bending fish body.

In fact, activation of the axial musculature by motor neurons in the central nervous system (CNS) can drastically, and transiently, alter body stiffness because muscle contraction places the myosepta and horizontal septum into tension, which increases intramuscular pressure (Wainwright, 1983; Long et al., 1996). In addition, it is likely that the precise motor pattern (that is, the exact magnitude and duration of muscle activation) produced will dynamically alter body flexural stiffness during the behavior, which, in turn, will alter the magnitude of the elastic energy that is stored and released. It is also clear that the CNS coordinates axial muscle activity during stage 2 to generate an effective takeoff angle – that is, to produce a takeoff angle that enables a jumping fish to enter into horizontally directed ballistic flight (Gibb et al., 2013). Electromyograms from multiple species with varying terrestrial locomotor abilities will ultimately be necessary to determine how fish generate effective terrestrial movements.

However, fundamental aspects of the functional anatomy of self-stranding teleosts remain unexamined. For example, it is possible there is variation in myotomal morphology among species with different terrestrial abilities. How might myotomal morphology enhance transmission of forces to the tail on land vs. in water? When jumping and non-jumping species are compared,

is there variation in the arrangement of the connective tissues comprising the myosepta, horizontal and vertical septa? Consider the unusual projections that form a second neural arch on the vertebrae of *K. marmoratus* (Fig. 7); do these or other as-yet-to-be-examined aspects of vertebral morphology enhance energy storage by the body and/or force transmission to the tail?

Ongoing work in our laboratories will address these and other questions related to possible anatomical and neurobiological features that allow fish to leave their aquatic habitat and move into a novel environment: the terrestrial realm. We anticipate that progress in understanding the biomechanical basis of terrestrial movements by teleost fishes will generate key insights into fundamental principles governing the interaction of stiff and pliant tissues that cooperate to produce explosive behaviors in highly flexible structures. Such understanding will facilitate advances in the diverse fields of biomimetic robotics, prosthetic design, and evolutionary biomechanics.

Acknowledgements

We thank the organizers of the symposium “Axial systems and their actuation: new twists on the ancient body of vertebrates” held at the 2013 International Congress of Vertebrate Morphology, for the invitation to be part of this special issue. We are indebted to Sandy Kawano and Richard Blob for assistance with ground-reaction force measurements, and Cinnamon Pace for assistance with video recording. We also thank two anonymous reviewers for providing comments that aided us in improving the manuscript. This work was supported by the National Science Foundation (grant no. IOS-0922605 and IOS-1306718).

Appendix A. Supplementary data

Supplementary material related to this article can be found, in the online version, at <http://dx.doi.org/10.1016/j.zool.2013.10.005>.

References

- Ashley-Ross, M.A., 1994. Hindlimb kinematics during terrestrial locomotion in a salamander (*Dicamptodon tenebrosus*). *J. Exp. Biol.* 193, 255–283.
- Bayliss, J.R., 1982. Unusual escape response by two cyprinodontiform fishes, and a bluegill predator's counter-strategy. *Copeia* 1982, 455–457.
- Bhalla, A.P.S., Griffith, B.E., Patankar, N.A., 2013. A forced damped oscillation framework for undulatory swimming provides new insights into how propulsion arises in active and passive swimming. *PLoS Comput. Biol.* 9, e1003097.
- Butcher, M.T., Blob, R.W., 2008. Mechanics of limb bone loading during terrestrial locomotion in river cooter turtles (*Pseudemys concinna*). *J. Exp. Biol.* 211, 1187–1202.
- Carpenter-Carter, S., Perlman, B.M., Ashley-Ross, M.A., 2012. Jumping performance of largemouth bass (*Micropterus salmoides*) across a size gradient. *Integr. Comp. Biol.* 52 (Suppl. 1), 222 (Abstract).
- Conte, J., Modarres-Sadeghi, Y., Watts, M.N., Hover, F.S., Triantafyllou, M.S., 2010. A fast-starting mechanical fish that accelerates at 40 m s⁻². *Bioinspir. Biomim.* 5, 1–9.
- Costa, W.J.E.M., 1998. Phylogeny and classification of the Cyprinodontiformes (Euteleostei: Atherinomorpha): a re-appraisal. In: Malabarba, L.R., Reis, R.E., Vari, R.P., Lucena, Z.M.S., Lucena, C.A.S. (Eds.), *Phylogeny and Classification of Neotropical Fishes*. EDIPUCRS, Porto Alegre, pp. 537–560.
- Costa, W.J.E.M., 2012. The caudal skeleton of extant and fossil cyprinodontiform fishes (Teleostei: Atherinomorpha): comparative morphology and delimitation of phylogenetic characters. *Vert. Zool.* 62, 161–180.
- Daan, S., Belterman, T., 1968. Lateral bending in locomotion of some lower tetrapods. *Proc. Ned. Akad. Wetten C* 71, 245–266.
- Davis, W.P., Taylor, D.S., Turner, B.J., 1990. Field observations on the ecology and habits of the mangrove rivulus (*Rivulus marmoratus*) in Belize and Florida. *Ichthyol. Explor. Freshwaters* 1, 123–134.
- Dickinson, M.H., Farley, C.T., Full, R.J., Koehl, M.A.R., Kram, R., Lehman, S., 2000. How animals move: an integrative view. *Science* 288, 100–106.
- Dingerkus, G., Uhler, L.D., 1977. Enzyme clearing of Alcian Blue stained whole small vertebrates for demonstration of cartilage. *Biotech. Histochem.* 52, 229–232.
- Domenici, P., Blake, R.W., 1997. The kinematics and performance of fish fast-start swimming. *J. Exp. Biol.* 200, 1165–1178.
- Eaton, R.C., Lee, R.K.K., Foreman, M.B., 2001. The Mauthner cell and other identified neurons of the brainstem escape network of fish. *Prog. Neurosci.* 63, 467–485.
- Esposito, C.J., Tangorra, J.L., Flammang, B.E., Lauder, G.V., 2012. A robotic fish caudal fin: effects of stiffness and motor program on locomotor performance. *J. Exp. Biol.* 56–67.
- Fish, F.E., 1998. Comparative kinematics and hydrodynamics of odontocete cetaceans: morphological and ecological correlates of swimming performance. *J. Exp. Biol.* 201, 2867–2877.
- Fish, F., Lauder, G.V., 2013. Not just going with the flow. *Am. Sci.* 101, 114–123.
- Frolich, L.M., Biewener, A.A., 1992. Kinematic and electromyographic analysis of the functional role of the body axis during terrestrial and aquatic locomotion in the salamander *Ambystoma tigrinum*. *J. Exp. Biol.* 162, 107–130.
- Gans, C., 1962. Terrestrial locomotion without limbs. *Am. Zool.* 2, 167–182.
- Gibb, A.C., Ashley-Ross, M.A., Pace, C.M., Long Jr., J.H., 2011. Fish out of water: terrestrial jumping by fully aquatic fishes. *J. Exp. Zool. A* 315, 649–653.
- Gibb, A.C., Ashley-Ross, M.A., Hsieh, S.T., 2013. Thrash, flip or jump: the behavioral and functional continuum of terrestrial locomotion in teleost fishes. *Integr. Comp. Biol.* 53, 295–306.
- Gillis, G.B., 1997. Anguilliform locomotion in an elongate salamander (*Siren intermedia*): effects of speed on axial undulatory movements. *J. Exp. Biol.* 200, 767–784.
- Hale, M.E., Long Jr., J.H., McHenry, M.J., Westneat, M.W., 2002. Evolution of behavior and neural control of the fast-start escape response. *Evolution* 56, 993–1007.
- Hebrank, J.H., Hebrank, M.R., Long Jr., J.H., Block, B.A., Wainwright, S.A., 1990. Backbone mechanics of the blue marlin, *Makaira nigricans* (Pisces, Istiophoridae). *J. Exp. Biol.* 148, 449–459.
- Hildebrand, M., 1985. Walking and running. In: Hildebrand, M., Bramble, D.M., Liem, K.F., Wake, D.B. (Eds.), *Functional Vertebrate Morphology*. Belknap Press, Cambridge, MA, pp. 38–57.
- Huehner, M.K., Schramm, M.E., Hens, M.D., 1985. Notes on the behavior and ecology of the killifish *Rivulus marmoratus* Poey 1880 (Cyprinodontidae). *Fla. Scientist* 48, 1–6.
- Jayne, B.C., 1985. Swimming in constricting (*Elaphe g. guttata*) and nonconstricting (*Nerodia fasciata pictiventris*) colubrid snakes. *Copeia* 1985, 195–208.
- Jayne, B.C., Lauder, G.V., 1993. Red and white muscle activity and kinematics of the escape response of bluegill sunfish during swimming. *J. Comp. Physiol. A* 173, 495–508.
- Kawano, S.M., Blob, R.W., 2013. Propulsive forces of mudskipper fins and salamander limbs during terrestrial locomotion: implications for the invasion of land. *Integr. Comp. Biol.* 53, 283–294.
- Koob, T.J., Long Jr., J.H., 2000. The vertebrate body axis: evolution and mechanical function. *Amer. Zool.* 40, 1–18.
- Long Jr., J.H., 1992. Stiffness and damping forces in the intervertebral joints of blue marlin (*Makaira nigricans*). *J. Exp. Biol.* 162, 131–155.
- Long Jr., J.H., 1998. Muscles, elastic energy, and the dynamics of body stiffness in swimming eels. *Am. Zool.* 38, 771–792.
- Long Jr., J.H., Nipper, K.S., 1996. The importance of body stiffness in undulatory propulsion. *Am. Zool.* 36, 678–694.
- Long Jr., J.H., McHenry, M.J., Boetticher, N.C., 1994. Undulatory swimming: how traveling waves are produced and modulated in sunfish (*Lepomis gibbosus*). *J. Exp. Biol.* 192, 129–145.
- Long Jr., J.H., Hale, M.E., McHenry, M.J., Westneat, M.W., 1996. Functions of fish skin: flexural stiffness and steady swimming of longnose gar, *Lepisosteus osseus*. *J. Exp. Biol.* 199, 2139–2151.
- Long Jr., J.H., Koob-Emunds, M., Sinwell, B., Koob, T.J., 2002. The notochord of hagfish, *Myxine glutinosa*: viscoelastic properties and mechanical functions during steady swimming. *J. Exp. Biol.* 205, 3819–3831.
- Long Jr., J.H., Porter, M.E., Liew, C.W., Root, R.G., 2010. Go reconfigure: how fish change shape as they swim and evolve. *Integr. Comp. Biol.* 50, 1120–1139.
- Long Jr., J.H., Krenisky, N.M., Roberts, S.F., Hirokawa, J., de Leeuw, J., Porter, M.E., 2011a. Testing biomimetic structures in bioinspired robots: how vertebrae control the stiffness of the body and the behavior of fish-like swimmers. *Integr. Comp. Biol.* 51, 158–175.
- Long Jr., J.H., Koob, T., Schaefer, J., Summers, A., Bantilan, K., Grotmol, S., Porter, M.E., 2011b. Inspired by sharks: a biomimetic skeleton for the flapping, propulsive tail of an aquatic robot. *Mar. Tech. Soc. J.* 45, 119–129.
- Mast, S.O., 1915. The behavior of *Fundulus*, with especial reference to overland escape from tide-pools and locomotion on land. *J. Anim. Behav.* 5, 341–350.
- McHenry, M.J., Pell, C.A., Long Jr., J.H., 1995. Mechanical control of swimming speed: stiffness and axial wave form in an undulatory fish model. *J. Exp. Biol.* 198, 2293–2305.
- McHenry, M.J., Azizi, E., Strother, J.A., 2003. The hydrodynamics of locomotion at intermediate Reynolds numbers: undulatory swimming in ascidian larvae (*Botrylloides* sp.). *J. Exp. Biol.* 206, 327–343.
- Nowroozi, B.N., Brainerd, E.L., 2013. X-ray motion analysis of the vertebral column during the startle response in striped bass, *Morone saxatilis*. *J. Exp. Biol.* 216, 2833–2842.
- Parenti, L.R., 1981. A phylogenetic and biogeographic analysis of cyprinodontiform fishes (Teleostei, Atherinomorpha). *Bull. Am. Mus. Nat. Hist.* 168, 335–557.
- Perlman, B.M., Kawano, S., Blob, R.W., Ashley-Ross, M.A., 2013. Citius, altius, fortius: jumping kinematics and kinetics in two distantly related teleosts. *Integr. Comp. Biol.* 53 (Suppl. 1), e165 (Abstract).
- Pfeifer, R., Bongard, J.C., 2007. *How the Body Shapes the Way We Think: A New View of Intelligence*. MIT Press, Cambridge, MA.

- Pfeifer, R., Iida, F., Gabriel Gómez, G., 2006. Morphological computation for adaptive behavior and cognition. *Int. Congress Series* 1291, 22–29.
- Rasband, W.S., 1997–2012. ImageJ. U.S. National Institutes of Health, Bethesda, MD, USA, <http://imagej.nih.gov/ij/>
- Ritter, D., 1992. Lateral bending during lizard locomotion. *J. Exp. Biol.* 173, 1–10.
- Root, R.G., Courtland, H.-W., Shepherd, W., Long Jr., J.H., 2007. Flexible flapping fish: periodic and secular body reconfigurations in swimming lamprey, *Petromyzon marinus*. *Exp. Fluids* 43, 779–797.
- Ryerson, W.G., 2013. Jumping in the salamander *Desmognathus ocoee*. *Copeia* 2013, 512–516.
- Sfakiotakis, M., Lane, D.M., Davies, J.B.C., 1999. Review of fish swimming modes for aquatic locomotion. *IEEE J. Oceanic Engr.* 24, 237–252.
- Soares, D., Bierman, H.S., 2013. Aerial jumping in the Trinidadian guppy (*Poecilia reticulata*). *PLOS ONE* 8, e61617.
- Summers, A.P., Long Jr., J.H., 2006. Skin and bones, sinew and gristle: the mechanical behavior of fish skeletal tissues. In: Shadwick, R.E., Lauder, G.V. (Eds.), *Fish Biomechanics*, vol. 23: Fish Physiology. Academic Press, San Diego, pp. 141–177.
- Taylor, D.S., 1990. Adaptive specializations of the cyprinodont fish *Rivulus marmoratus*. *Fla. Scientist* 53, 239–248.
- Tytell, E.D., Lauder, G.V., 2002. The C-start escape response of *Polypterus senegalus*: bilateral muscle activity and variation during stage 1 and 2. *J. Exp. Biol.* 205, 2591–2603.
- Tytell, E.D., Hsu, C.-Y., Williams, T.L., Cohen, A.H., Fauci, L.J., 2010. Interactions between body stiffness, muscle activation, and fluid environment in a neuromechanical model of lamprey swimming. *Proc. Natl. Acad. Sci. U. S. A.* 107, 19832–19837.
- Wainwright, S.A., 1983. To bend a fish. In: Webb, P., Weihs, D. (Eds.), *Fish Biomechanics*. Praeger Publ., New York, pp. 68–91.
- Webb, J.E., 1973. The role of the notochord in forward and reverse swimming and burrowing in the amphioxus *Branchiostoma lanceolatum*. *J. Zool.* 170, 325–338.
- Webb, P.W., 1975. Hydrodynamics and energetics of fish propulsion. *Bull. Fish. Res. Bd. Can.* 190, 1–159.
- Westneat, M.W., Hale, M.E., McHenry, M.J., Long Jr., J.H., 1998. Mechanics of the fast-start: muscle function and the role of intramuscular pressure in the escape behavior of *Amia calva* and *Polypterus palmas*. *J. Exp. Biol.* 201, 3041–3055.
- Zottoli, S.J., Faber, D.S., 2000. The Mauthner cell: what has it taught us? *Neuroscientist* 6, 26–38.